# Maximum Power Point Tracking for a Wind Turbine

By

Alec Biesterfeld

Tyler Rasmussen

Ben Scrementi

Final Report for ECE 445, Senior Design, Fall 2018

TA: Evan Widloski

December 12, 2018

Project No. 11

## Abstract

The following report presents our findings in creating a maximum power point tracking device for a medium-sized wind turbine. The solution uses a power converter and a digital controller to algorithmically determine the point of maximum power extraction given a particular wind condition. In determining the point of maximum power point, our system implements an iterative approach in which the controller tests a series of duty cycle as it converges to a duty cycle at which maximum power dissipation through a load resistor occurs. In addition, our system presents the user with specifications that include efficiency and output power delivered to the load. This report documents the motivation, design, verification, and final results of the maximum power point tracking solution.

# Contents

# 1 Introduction

## 1.1 Purpose

As the world races to reduce emissions and satisfy ever-increasing energy demands, many people debate the appropriate actions needed to supply the world's future energy needs. With global energy demand expected to increase by nearly 30 % in the next 12 years, many experts anticipate that much of the world, especially in developing regions, must transition to a microgrid approach where energy systems generate and utilize locally generated electricity as opposed to relying on a grid-based infrastructure that dominates electric power distribution today. One barrier inhibiting the deployment of microgrid systems on a larger scale relates to the costs of implementation as well as the availability of accessible solutions for harvesting renewable energy on a smaller scale. For our contribution to solving this problem, we sought to develop a low-cost and effective system that maximizes power extraction from the WindTura 750, a microgrid-scale wind turbine provided to our team for the project.

While various maximum power point trackers exist on the market today, wind power point trackers tend to focus on maximum power point tracking in order to charge a battery bank rather than extract energy for immediate use. Our solution seeks to differentiate itself by finding the point of maximum power extraction and dissipating the energy into a resistive load, which allows us to simulate the immediate use or delivery of the energy harvested from the turbine. In a full microgrid implementation, our solution could be used to extract the maximum available energy and then an inverter could be used to supply excess energy to the local electric grid. Also, many maximum power point tracking solutions for turbines similar in size to the WindTura 750 that generate up to 800 W cost in excess of $400. Therefore, our project seeks to lower this cost to approximately $200 in order to accelerate the transition to smaller scale electrical generation.

## 1.2 Objectives

- The system must actively adjust the load presented to the turbine using a variable DC/DC converter duty cycle to achieve maximum power extraction.
- The system must be able to reliably deliver up to 800 W to the load given sufficient wind.
- Overall system (from turbine output to the load) can operate with an efficiency of 85 % or higher when operating at up to 100 W, 80 % at 100-300 W, and 75% or higher at 300-800 W.
- Our solution must have a viable market cost of less than $200 to provide a significant reduction in the current market cost.

## 1.3 Design Overview

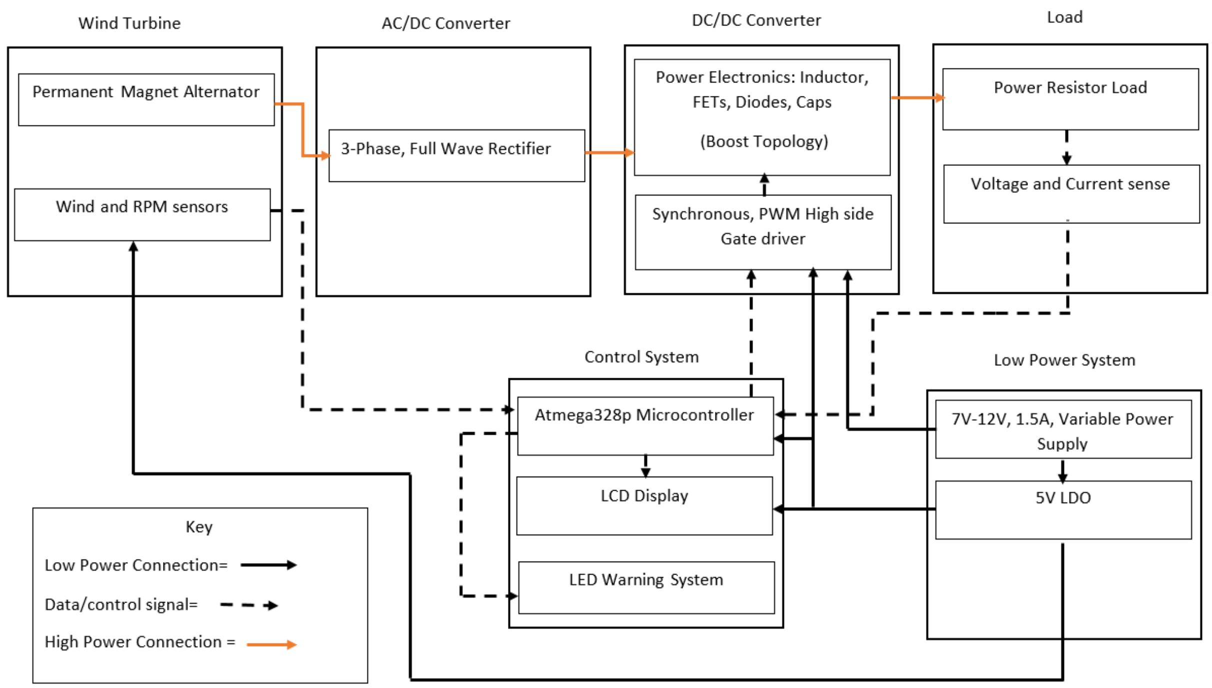


Figure 1: High-level Systems Block Diagram of Our Project

Our systems level design illustrated in figure 1 outlines our solution used to create a system capable of extracting maximum power from the WindTura 750 wind turbine. For the high power elements of our system, we connect the output of the wind turbine's permanent magnet alternator to a three-phase, full-wave rectifier that supplies the DC/DC converter with a direct current signal. The DC/DC converter then supplies the load resistor with the output power of the system to complete the high-power flow. In order to achieve maximum power extraction using the power electronics in our design, the control subsystem includes a microcontroller that supplies a variable duty cycle to the DC/DC subsystem, which allows us to vary the load presented to the turbine system and hence control the speed of the turbine to achieve maximum power point tracking.

Aside from the high-power requirements of our system, our block diagram has several low power subsystems and subblocks to support the MPPT functionality. This includes sensor units in the wind turbine and load subsystem blocks to allow the microcontroller to utilize pertinent system data such as output voltage, output current, wind speed, and rotational velocity of the wind turbine, which contribute data used to calculate power and efficiency data in the software running on the microcontroller. When the microcontroller finishes processing input from the sensor units present in figure 1, the data is displayed on the system display unit in the control system sub-block and the microcontroller blinks an LED to indicate that the system is operational. Finally, the diagram in figure 1 includes a low-power system to supply the microcontroller, sensors, system display, and gate driver circuit with 5 V and 7 V power connections that the individual components require to operate.

# 2 Design

## 2.1 AC/DC Converter

The AC/DC converter functions by converting the three-phase, alternating current output from the wind turbine's permanent magnet alternator into a direct current signal to supply the DC/DC converter subsystem. We implemented the AC/DC converter as a passive rectifier comprised of six diodes to achieve full-wave rectification and minimize diode conduction losses with the schematic presented in figure 2. The diodes were chosen such that each diode could sustain a continuous current of 25 A, which allows a total of 75 A of current to pass across the three phases of the rectifier circuit. Since we specified our system to handle up to 40 A of current in the design document, the chosen diodes are sufficient for this subsystem design. The full wave rectifier topology also enables us to achieve ripple below 20 % to supply the DC/DC subsystem with an appropriate DC signal, which we confirm using LTSPICE simulations with results shown in figure 3. Appendix B details the final layout of the AC/DC converter PCB.

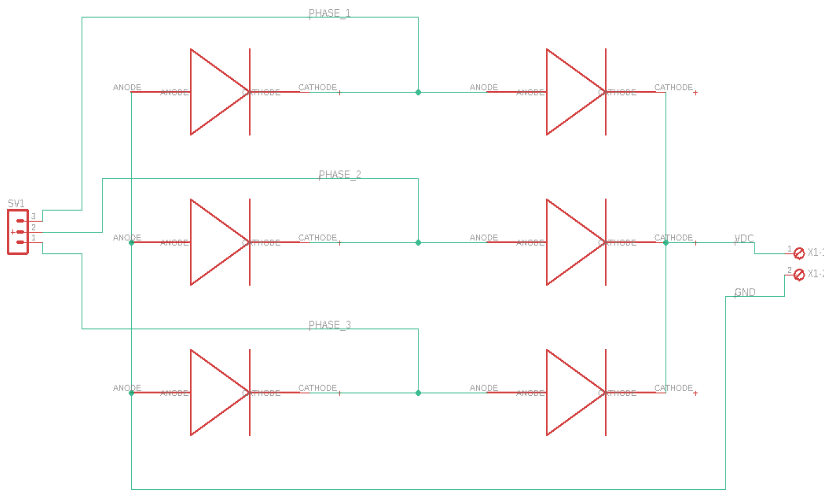


Figure 2: Eagle Schematic of the AC/DC Subsystem PCB

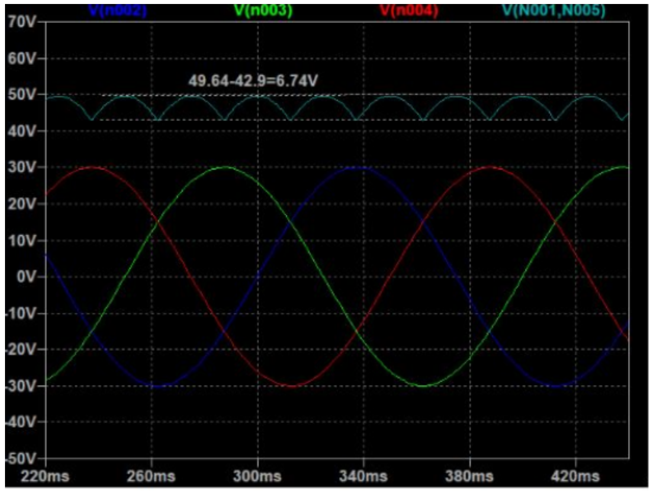


Figure 3: LTSPICE Simulation Results for the AC/DC Converter

## 2.2 DC/DC Converter

The DC/DC converter adjusts the load presented to the turbine by adjusting the output voltage. If the output voltage increases, then the load presented to the turbine is smaller and the turbine spins slower. If the output voltage decreases, then the load presented to the turbine is larger, and the turbine spins faster. The optimal speed can be found by adjusting the duty ratio of a DC/DC converter to adjust the load properly

### 2.2.1 Gate Driver

A gate driver is necessary in our design because the PWM signal from the microcontroller could only output up to 10 mA of current. A gate driver can take a PWM signal as an input and output the same signal with a higher current. If we were operating at 62.5 kHz, which is the default PWM signal duty ratio at the output of the microcontroller, then we would want the rise time of the gate voltage signal to be below 5 % of the corresponding period. Equation 1 shows the required current for a given rise time and gate charge of a MOSFET. Using our rise time of 0.8 $\mu$s and gate charge of 232 nC, we calculated the typical gate current to be 0.29 A [9]. We selected the LTC4442 because it was capable of outputting up to 1.5 A according to its datasheet [10].

$$I = \frac{Q_g}{t_r} \tag{1}$$

### 2.2.2 Boost Converter

We selected a boost converter for our design because it boosts the input voltage up. if our system were to be used to charge a battery, then at low wind speeds the output would not be able to charge a battery because the voltage would be too low. An ideal boost converter has the input-output voltage relationship shown in equation 1. At high duty ratios, the MOSFET is on more, and the output voltage is increased. At a duty ratio of 0 %, the output and input voltages are the same.

$$\frac{V_{out}}{V_{in}} = \frac{1}{1-D} \tag{2}$$

We followed Texas Instruments design guide to determine the minimum required inductor and capacitor values for our boost converter [14]. When we sized our components, we used an operating point with the maximum expected power of about 960 W. We used a 24 V input, 48 V output, and 2.4 Ω load. This operating point is higher than what we would see in our design, but allows us to have a margin of safety in our component selections. We chose our MOSFET and diode to comply with these higher voltages and currents. First, we calculated the current ripple going through the inductors and capacitors to be 18 A using equation 3. Because there is such a high current ripple, we had to select capacitors capable of operating with a high RMS current ripple. Using equation 4, we calculated our minimum capacitance to be 1.6 mF. The capacitors we ordered for our first-pass DC/DC converter were were 1.2 mF each, and were rated for 6.3 $A_{rms}$ of current ripple. To allow for a margin of safety, we used four of the capacitors in parallel, for a total capacitance of 4.8 mF and 25.2 $A_{rms}$ of current ripple. Our minimum inductance was found to be 16 mH using equation 5. We chose to use 20 mH for our inductance value.

$$\Delta I_L = 0.3 I_{out,max} \frac{V_{out}}{V_{in}} \tag{3}$$

$$C_{out} = \frac{I_{out,max} D}{f_s \Delta V_{out}} \tag{4}$$

$$L = \frac{V_{in}(V_{out} - V_{in})}{\Delta I_L f_s V_{out}} \tag{5}$$

Next, we simulated our gate driver and boost converter in LTSPICE, as shown in figure 4. Figure 5 shows the gate voltage, input voltage, output voltage, and capacitor current ripple in the simulation for the operating point described previously. We verified it was operating correctly and that the ripple, as shown in figure 6, was minimal. In the simulation, we achieved an output ripple of just 24 mV for a 42 V output.

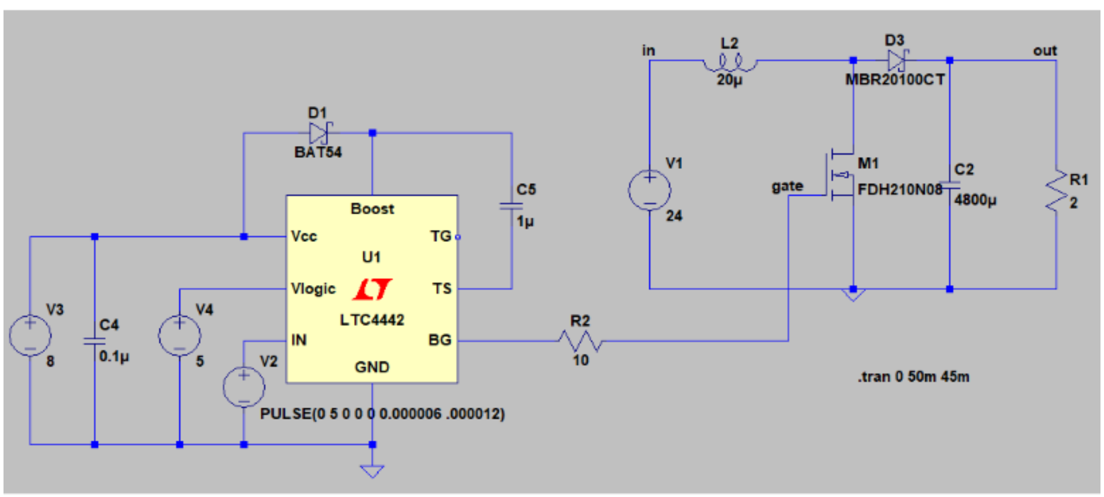


Figure 4: Schematic of the gate driver and boost converter simulation in LTSPICE

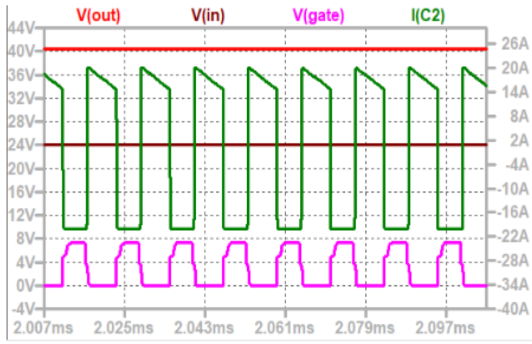


Figure 5: LTSPICE simulation results showing the gate voltage, input voltage, output voltage, and capacitor current ripple

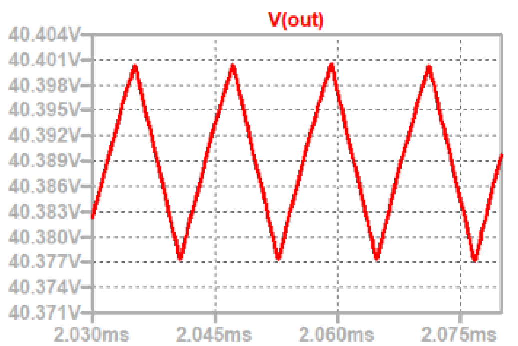


Figure 6: Output voltage in LTSPICE showing the voltage ripple of 24 mV

After we verified that our gate driver and boost converter were working correctly in LTSPICE, we created a schematic of our DC/DC converter PCB. It is shown in figure 7. The board layout is shown in appendix C. In order to dissipate more heat going through the MOSFET and diode, we added metal heatsinks to their package, which allowed us to operate at higher power without violating component temperature ratings.

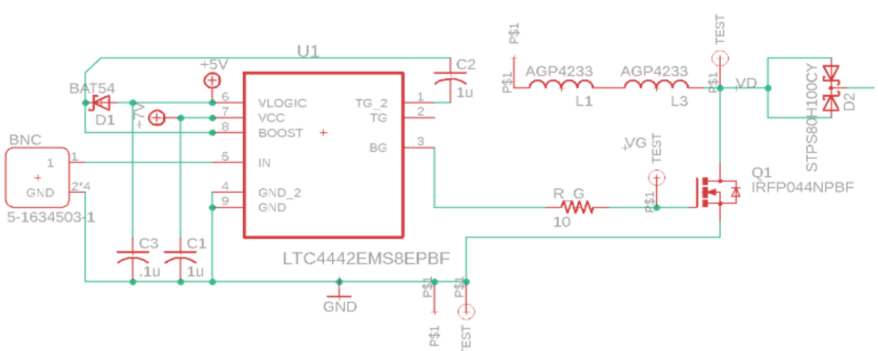


Figure 7: EAGLE schematic of the DC/DC converter PCB

## 2.3 Control System and Sensor Subsystems

The control system block in the high-level block diagram houses the microcontroller, LCD display, and the LED warning light because each of those sublocks were designed to be placed on the PCB itself. However, the control system design section also includes the low power supply and sensor units since these components interface directly with our microcontroller PCB, shown in figure 8, despite their placement within other subsystem blocks on the block diagram. Appendix D details the final layout of the control system PCB.

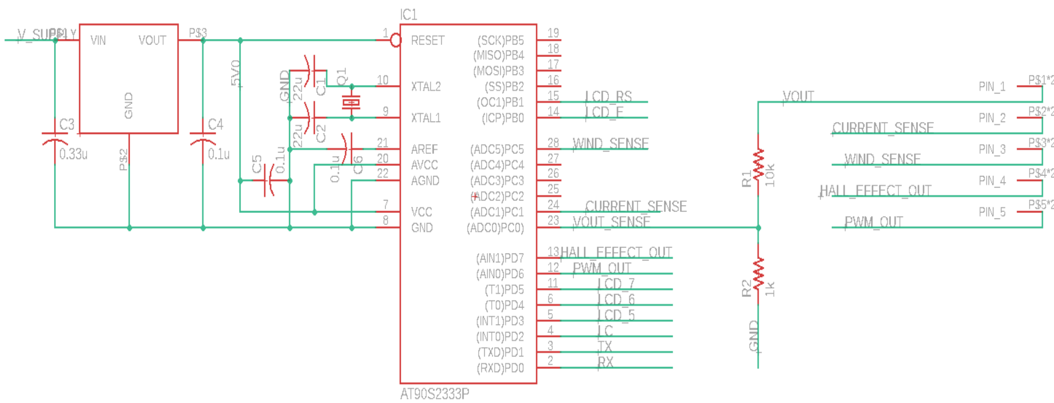

Figure 8: EAGLE schematic of the Control System PCB

### 2.3.1 Microcontroller

The microcontroller serves as a computational core that allows us to process data and issue control signals to other system components. In order implement the proposed functionality of our system, the ATMEGA328P provides the necessary analog-to-digital, and digital input-output functions that our systems demands, which serves as the primary reason for choosing this particular microcontroller in our design [12]. The pinout in appendix E demonstrates the necessary design functions supported by the pins available on the ATMEGA328P.

### 2.3.2 Wind and RPM Sensors

The wind and RPM sensors serve as a means to measure the wind speed and the mechanical power available to the system as well as verifying the varying rotational speed of the turbine for a change in duty cycle at the DC/DC converter. The wind sensor or anemometer generates an analog voltage value proportional to the wind speed. In software, we employed the lookup-table provided by the anemometer's manufacturer to convert the analog voltage value into a wind speed that could be stored on the microcontroller's dynamic memory.

We designed the RPM sensors using a digital hall-effect sensor and a neodymium magnet attached to the turbine blade. When the magnet passes the hall-effect sensor, the sensor will output a logic high to the microcontroller's digital input-output pin. The software responsible for calculating the turbine's rotational velocity looks for two consecutive rising edges at the digital input-output pin connected to hall-effect sensor. The rotational speed can then be calculated using the following formula where T2 and T1 are the times, in minutes, of the second and first rising edges from the digital signal of the hall-effect sensor output respectively.

$$RPM = \frac{1}{T2 - T1} \tag{6}$$

### 2.3.3 Voltage and Current Sensors

The voltage and current sensors in our design serve as a means to calculate output power. We chose a simple resistor divider circuit comprised of a 3.3 $k\Omega$ and a 10 $k\Omega$ resistor to ensure the voltage presented to the microcontroller's analog-to-digital converter was less than 5 V, the maximum readable input for the ATMEGA328P. This means that the design can tolerate output voltages up to 22.5 V, which exceeds the maximum output voltage we found while testing the system. Equation 7 details the calculation of the voltage presented to the microcontroller input, and the software uses the set resistor values to calculate the output voltage and display the data to the user.

$$V_{adc} = \frac{3.3k\Omega}{13.3k\Omega} * V_{out} \tag{7}$$

For the final demonstration, we redesigned the current sensor using four, 0.5 W resistors with a resistance of 15 $\Omega$ because the output power in the industrial fan tests never exceeded 2 W. In higher power applications, we purchased a 50 A current sensing module with a resolution of 40 mV/A. However, due to the current levels of 0.5 A or less in the final demonstration, the current sensing module lacked the necessary resolution to differentiate current changes for a change in DC/DC converter duty cycle, so the current sense resistors served as a design alternative. We determined the current at the output using the current sense resistors in series with the output load with the voltage across the current sense resistors determined using an analog-to-digital converter on the microcontroller. The current could then be calculated in software as the ratio of the voltage and the equivalent resistance of the current sensing unit as detailed in equation 8.

$$I_{out} = \frac{V_{adc}}{3.75\Omega} \tag{8}$$

### 2.3.4 System Display and LED Warning Light

The control subsystem processes the data and makes the system parameters available to the user through an LCD display unit. On the controller PCB, a light also flashes to warn people in the vicinity of the power electronics and turbine are operational. For the LCD display, the data collected from the sensor units is stored using the dynamic memory available in the ATMEGA328P microcontroller. Then, the system software outputs the data to the display unit using digital input-output pins available on the microcontroller. Specifically, the LCD display unit requires 6 digital signals to supply four registers as well as control the enable and read-write signals on the LCD module.

When the hall effect sensor outputs a logic high value to the digital input-output on the microcontroller, the software will update a variable to indicate the generation of power and operation of the turbine blades. This results in a blinking LED that we control by toggling a digital output on the microcontroller between logic low and logic high during the time in which the system generates power.

### 2.3.5 Low Power Supply

We include a low power subsystem block in the design of the control unit since the microcontroller, sensor units, and system display all operate using a 5 V power connection, and the gate driver circuit requires an 8 V power connection as well. In this block, the wall outlet power supply supplies the gate driver and the low dropout regulator with an 8 V power connection up with up to 1.5 A of current. This current allows us to power the gate driver circuit with its maximum current draw of 1 A while supplying the 0.2 A of maximum current draw for the remainder of the low power components connected to the 5 V connection. The low dropout regulator supports a maximum current of 1.5 A to avoid any potential damages in the case of a short circuit while also having the capability to supply the system with its necessary power requirements.

## 2.4 Software Design

### 2.4.1 Maximum Power Point Tracking (MPPT) Algorithm

The goal of MPPT for a wind turbine is to maximize the coefficient of power ($C_p$) for a given tip speed ratio ($\lambda$ or TSR). The $C_p$ is the ratio between the power at the output of the turbine to the power from the wind, as shown in equation 9. The TSR is simply the ratio between the tangential velocity of the tip of the blades and the velocity of the wind, as shown in equation 10 .

$$C_p = \frac{P_{turbine,out}}{P_{wind}} \tag{9}$$

$$\lambda = \frac{v_{tip}}{v_{wind}} \tag{10}$$

An example of a typical $C_p$-$\lambda$ curve is shown in figure 9, which shows there is only one maximum in the curve. The maximum on the graph is where the maximum power output is achieved. We wanted our algorithm to find that operating point for our wind turbine at various wind speeds.

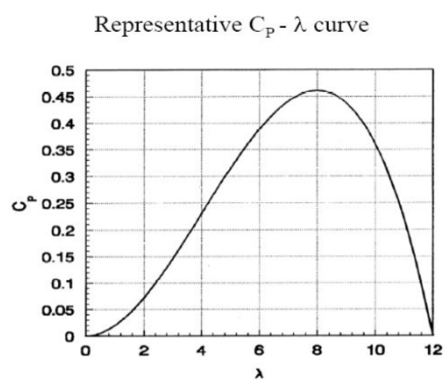


Figure 9: Typical $C_p$ - $\lambda$ curve for a constant wind speed

The flowchart depicted in figure 10 details the algorithm employed in our maximum power point tracking solution, which varies the duty cycle of the DC/DC converter until the optimal duty cycle for maximum power extraction is found. During the first iteration, the algorithm writes a 62.5 kHz PWM signal to the microcontroller's digital I/O pin connected to the DC/DC subsystem. Following the writing of a PWM signal, the system will not run the MPPT algorithm for 10 s to allow the turbine ample response time to adjust to the new load. After that, output power readings are collected and filtered over a 20 s sampling period in which 100 samples are collected to obtain an initial output power calculation. Following the first sampling period, the system increments the output duty cycle, delays operation for 10 s, and performs an identical output power sampling and filtering operation. If output power increased with an increase in the output duty cycle, the incremented duty cycle replaces the old default duty cycle value and the algorithm proceeds to the top of the control loop. Otherwise, the system will decrease the duty cycle at the output and perform the same delay and filtering sequences. If decrementing the duty cycle increases output power, the decremented value replaced the original duty cycle value and the algorithm proceeds to the top of the control loop. If not, the original duty cycle remains unchanged and the system will continue to adjust the duty cycle to avoid convergence at a local minimum and continue to adjust if wind conditions change.

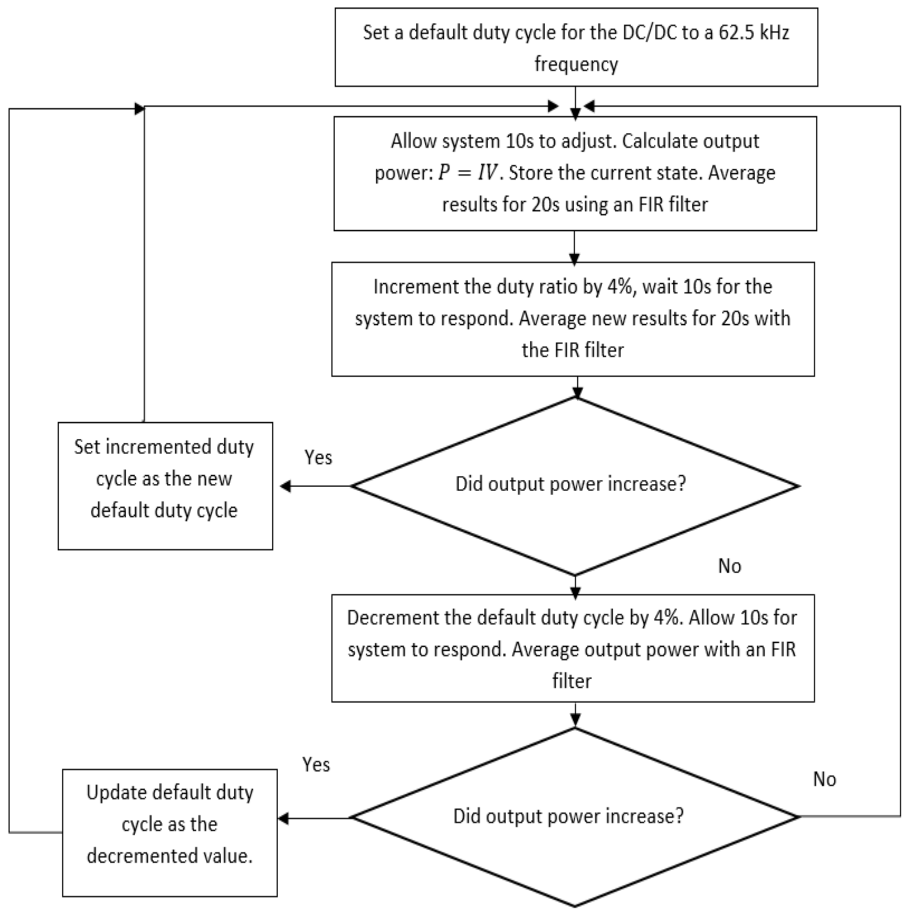


Figure 10: Software Flowchart outlining our MPPT Algorithm

# 3 Design Verification

The requirements for each module, as well as tests that could have been used to verify them independently, can be found in appendix A. However, because our system function properly as a whole in our demonstration, we did not need to run each individual test to verify the components.

## 3.1 AC/DC Converter

We verified the requirements of our AC/DC converter using a test setup consisting of the dynamometer, AC/DC converter, and a resistive load. The dynamometer supplied torque to the turbine's permanent magnet alternator which then provided a three-phase, alternating current input into our AC/DC subsystem. The AC/DC converter rectified the power and the load resistors dissipate the generated energy. We attached wattmeter to the output of the AC/DC converter while also employing the two-wattmeter method to measure input power such that the efficiency specifications could be measured. Table 1 summarizes the results of this verification test and figure 11 shows that the AC/DC converter fulfills its ripple requirement.

| RPM | Input Power (W) | Output Power (W) | $\eta$ (%) |
|---|---|---|---|
| 100 | 11.47 | 9.60 | 83.69 |
| 200 | 48.43 | 43.70 | 90.23 |
| 300 | 109.26 | 101.70 | 93.08 |
| 400 | 193 | 182 | 94.3 |

Table 1: Efficiency Data for the AC/DC converter with $R_{load}$=8Ω

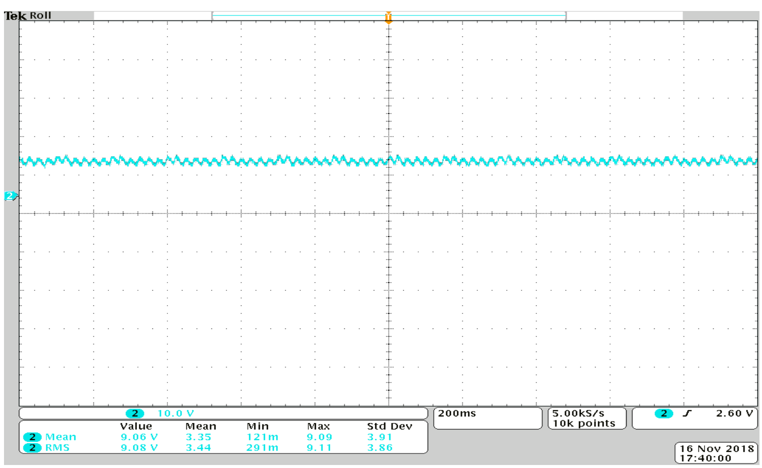


Figure 11: Scope Capture used to verify AC/DC Converter Ripple Requirements

## 3.2 DC/DC Converter

We tested our boost converter PCB at low power first. Our test setup involved a DC power supply as the input, a resistor box as a load, and power meters at the input and output of the boost converter. First we tested it at 90 W by setting the input voltage from a DC supply to 20 V, the duty ratio to around 30 % and the load resistor to 7 Ω. According to equation 1, we should expect the output voltage to be approximately 28 V. The observed output voltage was 25.1 V, which was about 10.7 % different from what it should have been for an ideal boost converter. The difference is due to voltage drops across the MOSFET and diode, as well as the equivalent series resistance, or

ESR, of the capacitors and inductors. According to our power meters, we achieved an efficiency of 91.8 % with 90.1 W at the output. This satisfies our 90 % efficiency requirement for the DC/DC converter at 100 W. We measured the voltage ripple to be 65 mV for this case, which is only 0.2 % of the output voltage. This is within our 3 % ripple requirement at 100 W. However, we had large voltage spikes at the output. We tuned our gate resistance to minimize them as best we could, and we chose a 110 Ω gate resistance after testing many options. For the 90 W operating point, the voltage spikes were as large as 3.9 V. This can be seen the oscilloscope capture in figure 12.


Figure 12: Oscilloscope capture of the boost converter's gate voltage and output voltage at 90 W.

We repeated the same test at a higher power operating point. We used a slightly higher load resistance of 8.33Ω, an input voltage of 38.2 V, and a duty ratio of 33.5 %. This resulted in 309 W at the output. The efficiency for this operating point was about the same at 91.6 %, and the output voltage ripple was about 80 mV. The efficiency and output voltage ripple were well within our required specifications of 85 % and ±5 % of the output voltage, respectively.

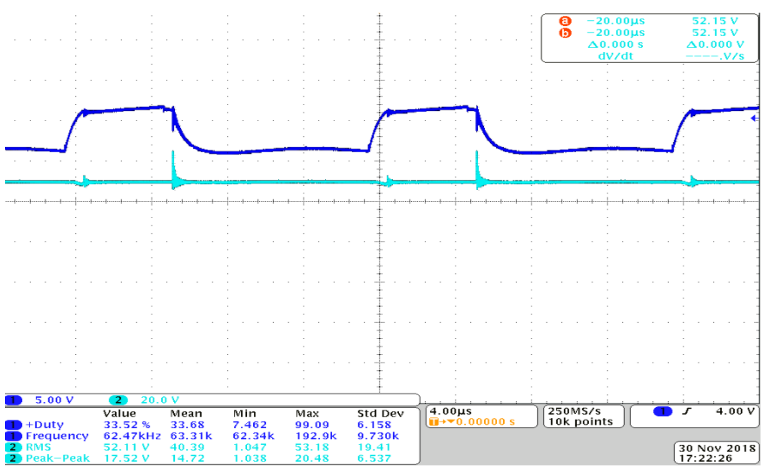


Figure 13: Oscilloscope capture of the boost converter's gate voltage and output voltage at 309 W.

Table 2 shows a summary of these two operating points used to verify our boost converter. Although our original requirements stated that our converter should be able to operate at 800 W, we only tested at up to 309 W because of thermal limitations. At 309 W, our MOSFET was reaching a temperature of 90 $^{\circ}C$, and the package was rated for 125 $^{\circ}C$. With each increase in output power at this point, the temperature was increasing rapidly, and we did not want to risk destroying our PCB with limited time remaining before our final demonstration.

| $R_{load}$ | 7Ω | 8.33Ω |
|---|---|---|
| Duty Ratio | 29 % | 33.5 % |
| $V_{in}$ | 19.63 V | 38.2 V |
| $P_{in}$ | 98.1 W | 37.6 W |
| $V_{out}$ | 25.1 V | 50.94 V |
| $P_{out}$ | 90.1 W | 309.4 W |
| $\eta$ | 91.8 % | 91.6 % |
| $V_{out}$ Spikes | 3.5 V | 14 V |
| $V_{out}$ Ripple | 65 mV | 79 mV |
| Required Ripple | 0.75 V | < 2.5 V |

Table 2: Summary of test data for the boost converter

## 3.3 Control System

We carried out our verification steps for the control system, including the sensor units, display, and low power units in two stages. First, we performed verification tests on the individual hardware and software pieces in the control system with the tabulated results presented in section 3.3. The second step involved full-systems testing and algorithm tuning using the industrial fan with results provided in section 3.5. In particular, appendix A details any qualitative verification results while section 3.3 will present the quantitative verifications of the control and sensor elements.

### 3.3.1 Wind and RPM Sensors Verification

Our anemometer reads the input wind speed to determine the mechanical power available to the turbine. Incorrect wind speed readings would result in incorrect power and efficiency calculations in the system software, so our verification step ensures that our anemometer setup reads the correct wind speed. In the verification test, we first uploaded the code onto our microcontroller to read the wind speed and output the data onto the LCD display unit. We then set the industrial fan speed to its low setting and compared the reading to the known value in the fan's datasheet to ensure that the wind sensor could accurately determine the wind speed in our final demonstration setup. After that, we repeated the test on the high fan speed to verify the accuracy requirement of the anemometer and test its ability to interface with the microcontroller and LCD display unit.

| **Fan Speed** | **Wind Speed (known)** | **Wind Speed (measured)** |
|---|---|---|
| Low | 1.13 m/s | 1.14 m/s |
| High | 4.53 m/s | 4.56 m/s |

Table 3: Anemometer Verification Results

The RPM sensor measures the rotational velocity of the turbine in revolutions-per-minute (RPM), which we verified using the dynamometer as a means to control the rotational speed of the turbine's alternator. Using the dynamometer control software, we set the rotational speed to a value of 100 RPM with the sensor unit connected to the microcontroller and LCD display unit with the software to calculate the RPM and control the LCD display. We then recorded the rotational speed our control system calculated and repeated the test for 200, 300, and 400 RPM to verify the accuracy of our sensor implementation.

| RPM (dynamometer) | RPM (LCD Display) |
|---|---|
| 100 | 100 |
| 200 | 201 |
| 300 | 302 |
| 400 | 398 |

Table 4: RPM Verification Results

### 3.3.2 Current and Voltage Sensors

The verification steps for the voltage sensor unit included uploading the software to the microcontroller used to calculate the voltage based on the analog-to-digital converter reading at the sensing node in the voltage divider circuit. Using a 25 V power supply, we applied a known voltage to the voltage sensing circuit and recorded the value displayed on the control system's LCD display to verify the sensor accuracy with results tabulated in table 5.

| Applied Voltage (V) | Measured Voltage on LCD Display (V) |
|---|---|
| 1 | 0.97 |
| 5 | 505 |
| 10 | 10.1 |
| 20 | 20.17 |

Table 5: Voltage Sensor Verification Results

The current sensor unit needed to have high accuracy due to the low-current operation in the final demonstration test setup. In order to verify its accuracy, the microcontroller and LCD display calculated and displayed the measured data processed by the system software while a DC power supply supplied a known current to the sensor unit. The results shown in table 6 provide the results.

| Voltage (V) | Supplied Current (A) | Measured Current LCD Display (A) |
|---|---|---|
| 0 | 0 | 0 |
| 0.1 | 0.027 | 0.028 |
| 0.2 | 0.053 | 0.052 |
| 0.3 | 0.08 | 0.08 |
| 0.4 | 0.106 | 0.11 |

Table 6: Current Sensor verification Results

### 3.3.3 Low Power Supply

In order to ensure the power supplied to the control subsystem never exceeded its maximum rating of 5.5 V, we tested the low power system for each of the variable wall-outlet supply's voltage settings. The voltages at the supply and output of the regulator were measured using a digital multimeter. Table 7 shows the results of the Low Power subsystem test.

## 3.4 Dynamometer Testing

We integrated the permanent magnet alternator, AC/DC converter, DC/DC converter, and resistive load together to test the alternator and power electronics at high power. Our test setup used a motoring dynamometer to drive our permanent magnet alternator at a specified torque. Its output was then fed into two power meters that would measure the power output using the two wattmeter method. The output of the power meters then went to our

| **Wall Supply Voltage (V)** | **Regulator Voltage Output (V)** |
|---|---|
| 8 | 4.987 |
| 9 | 4.989 |
| 10 | 4.997 |
| 11 | 4.998 |
| 12 | 4.998 |

Table 7: Low Power Verification Results

AC/DC converter and DC/DC converter. The output of the DC/DC converter was wired to another power meter and to a resistor box, which acted as the load. This test would simulate wind providing torque to the turbine, and the output going through our power electronics to the load.

We set the dynamometer to operate at 5.5 Nm with a 7 Ω or 14 Ω load at the output. We then adjusted the duty ratio of the DC/DC converter using a function generator to provide a PWM signal to the gate driver. We recorded data for a few different duty ratios and saw that as we increased the duty ratio, the boost converter decreased the load presented to the turbine, causing it to spin slower for the same torque. The data is shown in table 5. We met our efficiency requirement of 80 % at 122 W, 181 W, and 216 W. However, we did not meet our efficiency requirement of 85 % at less than 100 W. An example capture of the gate voltage and output voltage for the 187.7 W operating point is shown in figure 14. The voltage spikes from the DC/DC converter were reduced to approximately 2 V for a 55 V signal at the output.

| Load (Ω) | 7 | 7 | 7 | 14 | 14 | 14 |
|---|---|---|---|---|---|---|
| Duty Ratio (%) | 15 | 25 | 35 | 20 | 25 | 35 |
| Turbine Speed (RPM) | 270 | 210 | 160 | 434 | 380 | 268 |
| $P_{in}$ (W) | 113.2 | 84.2 | 57.7 | 216.0 | 181.8 | 122.4 |
| $V_{out}$ (V) | 26.1 | 22.0 | 17.7 | 50.8 | 47.2 | 37.5 |
| $P_{out}$ (W) | 97.0 | 68.9 | 44.7 | 187.7 | 156.9 | 101.4 |
| $\eta$(%) | 85.7 | 81.8 | 77.4 | 86.9 | 86.3 | 82.84 |
| Required $\eta$ (%) | 85 | 85 | 85 | 80 | 80 | 80 |

Table 8: Dynamometer testing data of the power electronics for different loads and duty ratios

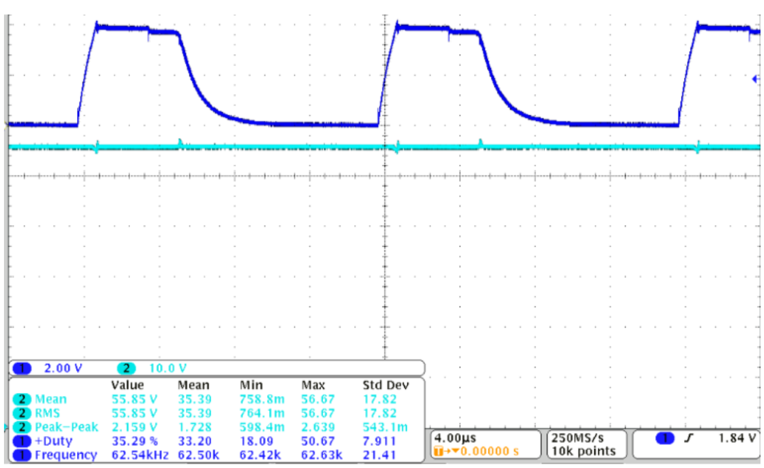


Figure 14: Oscilloscope capture of the gate voltage and output voltage of the system for the 187.7 W operating point

The dynamometer could only output a maximum power of 200 W, so we were unable to test our system at a little over 200 W for a few seconds before it would adjust to a lower speed. We were also unable to test our microcontroller's MPPT algorithm with the dynamometer because at a constant input torque, our converter would simply converge to the lowest duty ratio it can for all loads.

### 3.5 Fan Testing

To test our microcontroller's MPPT algorithm with our power electronics, we used an industrial fan to drive the full wind turbine with its blades attached. Because the fan provided actual airflow to drive the turbine, the aerodynamic properties that give rise to an optimal power point for the system were in effect.

Our test setup contained an industrial fan blowing on our turbine, and its output went to our AC/DC converter and DC/DC converter. Before connecting our microcontroller, we used a function generator to input a PWM signal into our DC/DC converter. With the fan running, we measured the output power using a power meter with the DC/DC converter at duty ratios every 4 % between 0 % and 80 %. We collected power meter data over the course of a minute after reaching steady state and took the average of the output power. We then plotted the relationship between steady state output power and the duty ratio in figure 15. We performed the test with the fan on its low and high speeds. Maximum power output was achieved at 48 % for the high speed and 36 % for the low speed. These points are indicated in figure 15 as well.

Next, we replaced the PWM signal from the function generator with the PWM output of our microcontroller PCB, so we could test our algorithm. We started with our system turned off, and the fan on its high speed setting. We allowed the turbine to reach a steady state output power, and then turned it on. Our algorithm started at an 8 % duty ratio, and took a little under eight minutes to converge between 40, 44, and 48 % duty ratios. The average duty ratio after it converged was around 43.5 %. After it converged, we switched the fan speed to low, and it took under three minutes to converge between 36, 40, and 44 % duty ratios. The average duty ratio after it converged was around 41.6 %. We plotted the output power and duty ratio of our system to display the algorithm's convergence in figure 16. The actual points where our algorithm converged are compared to our measured maximum power points in figure 16 as well. Our algorithm's converged duty ratios were different by 4.5 % and 5.6 % from the measured maximum power points for the high and low fan speed cases, respectively.

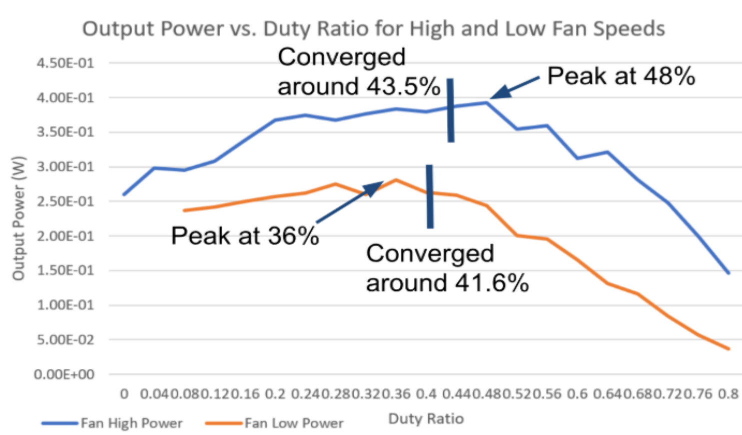


Figure 15: Collected data showing the relationship between output power and the duty ratio of the DC/DC converter

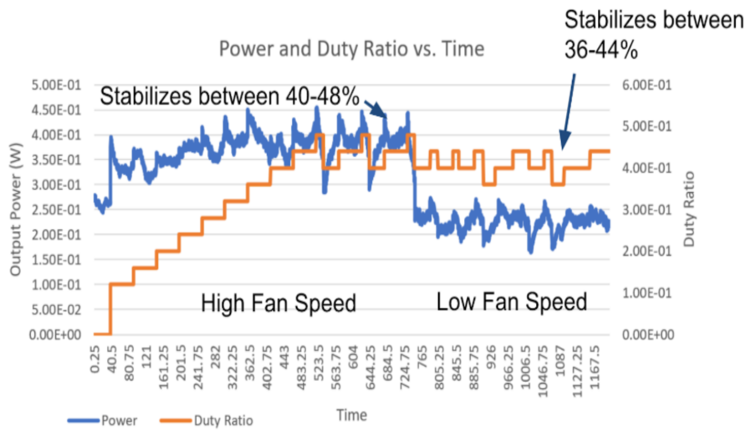


Figure 16: Data collected while our microcontroller was determining the optimal duty ratio at high and low fan speeds. Lines show the output power (W) and duty ratio

We were only able to achieve a maximum output of around 400 mW with this test setup. Despite operating at a low power, these tests prove that our system could determine the maximum power point of the system within a reasonable margin. The reason the system takes up to eight minutes to converge to the maximum power point is that the turbine's output power takes up to one minute to stabilize after changing the duty ratio by 4 %.

# 4 Cost

## 4.1 Parts

**Table 9: Parts Costs**

| Part | QTY | Retail Cost ($) | Cost in Bulk ($) |
|---|---|---|---|
| PCB's | 3 | 3 | 3 |
| LTC4442 Synchronous Gate Driver | 1 | 2.56 | 1.40 |
| High Power MOSFET | 1 | 9.16 | 5.68 |
| ATMEGA328P Microcontroller | 1 | 1.96 | 1.63 |
| Anemometer | 1 | 17.00 | 17.00 |
| LCD Display | 1 | 2.46 | 1.98 |
| Rectifier Diodes | 6 | 15.78 | 6.60 |
| Miscellaneous Passives | 1 | 2.78 | 1.17 |
| Inductor (10$\mu$H) | 2 | 35.30 | 20.36 |
| High Power Schottky Diode | 1 | 13.63 | 8.64 |
| Low Power Schottky Diode | 1 | 2.34 | 1.17 |
| Aluminum Capacitors (1200$\mu$F) | 4 | 26.20 | 18.64 |
| Crystal Oscillator | 1 | 0.74 | 0.57 |
| Hall Effect Sensor | 1 | 0.95 | 0.48 |
| High Current Sensor | 1 | 13.49 | 8.28 |
| Adjustable DC Power Supply | 1 | 9.98 | 9.98 |
| **Total** | | 157 | 107 |

## 4.2 Labor

Using the data from the ECE Illinois website, the average yearly salary for ECE undergraduates upon entering the workforce is approximately $75,625. This amount was determined by averaging the salary figures provided for electrical engineering ($67,000) and computer engineering ($84,250) students directly after graduation [8]. Taking this number into account with the standard 40 hour work week during a 52 week year, $75,625 translates into an hourly rate of approximately $36 per hour. As a calculation of the estimated total labor cost, we use equation 11 assuming each team member contributed approximately 100 hours to the project.

$$(3\ team\ members) * (100\ hours) * (\$36\ per\ hour) * 2.5 = \$27,000 \tag{11}$$

## 4.3 Schedule

Appendix F includes a table that provides a detailed outline of the project schedule and the division of work among team members.

# 5 Conclusion

## 5.1 Accomplishments

While we did not meet all of our high-level objectives, we still have accomplishments that are much worth sharing. We successfully demonstrated maximum power point tracking in a laboratory setting by spinning the turbine with wind from an industrial fan. The power electronics smoothly operated when coupled with the dynamometer and we met the 80 % efficiency specification for loads between 100 W and 300 W. Lastly, we completely integrated the active power converter with the WindTura 750 turbine system, all for under $200.

## 5.2 Uncertainties

One uncertainty we have is that we did not test our last DC/DC converter PCB at higher power because we did not want to risk burning a component with only one week until the final demonstration. Another issue we had was that our efficiency requirements should have been reversed. When we set the specifications, we set the higher efficiency specifications for lower power outputs, and we had the lowest efficiency requirement for high power output. The biggest uncertainty was that since we were only able to test the active power converter and wind turbine with the dynamometer and industrial fan, we have no data for how the system would perform at output power as high as the rated 800 W.

## 5.3 Ethical considerations

Since the wind turbine does have spinning blades, we established safety precautions in accordance with IEEE Code of Ethics, #9 [6]. We included a flashing LED to indicate that the turbine and power converters are operational so that any potential users can have a visual warning. During our demonstration, we placed barricades around the perimeter of the wind turbine to ensure that no one came within reach of the rotor blades.

Since we initially expected that our active power converter would have to handle up to 800 W being delivered to the load, we carefully selected parts that we were confident could handle the high amounts of current and voltage as well as temperature. We surrounded certain components with heat sinks to dissipate heat safely.

By keeping our budget for parts below $200, we hope that our design could make wind turbines made for the microgrid more accessible, as more than a billion people worldwide still live without electricity [7]. Coupled with the fact that our active power converter successfully tracked the maximum power point, we believe that our project can have an impact on so many lives.

## 5.4 Future work

We only got the chance to test the wind turbine with the dynamometer and the industrial fan in the senior design lab, so in the future creating better test conditions is a top priority . The dynamometer could not get the turbine motor to output the 800 W for which it is rated, and the industrial fan was delivering wind speeds well below the rated wind speed of 29 miles per hour. Placing the wind turbine in a wind tunnel or outside on a windy day would be more ideal since the wind turbine was designed for such environments. The results received from better test conditions would make it easier to characterize the turbine and develop more accurate models used for calculations and simulations.

Fine-tuning the power tracking algorithm will reduce delays that occur when trying to find the maximum power point. Less delays means that the duty ratio will converge to its optimal value faster, leading to a more hastily attained maximum output power. We could add a PID controller to improve response times. Battery integration is the next step for this project. A battery load would replace the resistive load to provide commercial viability to the design. The wind turbine will be able to charge the battery load and that can provide DC power for a multitude of purposes.

In our design document, we stated that we wanted to encase our active power converter to protect it from water. Another important component of future work would be to build such a case, especially if there is any testing conducted outside. The casing is essential to give the active power converter and mid-size turbines a chance at commercial success.

## References


[1] M. Froese, “An overview of 6 energy storage methods,” Windpower Engineering & Development, 26-Feb-2018. [Online]. Available: https://www.windpowerengineering.com/business-news-projects/uncategorized/an-overview-of-6-energy-storage-methods/. [Accessed: 15-Sep-2018].

[2] V. Boutin, M. Feasal, K. Cunic, and J. Wild, “How Microgrids Contribute to the Energy Transition,” Schneider Electric.

[3] O. Malik, “Micro-Grid: Concepts and Challenges in Practical Implementation,” IEEE Canadian Review, 2015.

[4] D. Milborrow, “At the tipping point: 2017 wind cost analysis,” Windpower Monthly, 01-Feb-2018. [Online]. Available: https://www.windpowermonthly.com/article/1455361/tipping-point-2017-wind-cost-analysis. [Accessed: 19-Sep-2018].

[5] Windynation.com, Tip Speed Ratio: How to Calculate and Apply TSR to Blade Selection. [online] Available: https://www.windynation.com/jzv/inf/tip-speed-ratio-how-calculate-and-apply-tsr-blade-selection [Accessed 17 Sep. 2018].

[6] Ieee.org,"IEEE IEEE Code of Ethics", 2018. [Online]. Available: http://www.ieee.org/about/corporate [Accessed: 16- Sept- 2018]

[7] GE.com, “More Than 1 Billion People Live Without Electricity. Here’s How We Turn Their Lights On”, 2016. [Online]. Available: https://www.ge.com/reports/more-than-a-lightbulb/ [Accessed: 16-Sept-2018]

[8] ece.illinois.edu, “Salary Averages,” Salary Averages :: ECE ILLINOIS. [Online]. Available: https://ece.illinois.edu/admissions/why-ece/salary-averages.asp. [Accessed: 29-Sep-2018].

[9] IXYS, “X3-Class HiPerFET Power MOSFET,” IXFP72N30X3/IXFQ72N30X3/IXFH72N30X3 datasheet, 2018. Available: http://ixapps.ixys.com/DataSheet/DS100853B(IXFP-FQ-FH72N30X3).pdf

[10] Linear Technology, “High Speed Synchronous N-Channel MOSFET Drivers,” LTC4442/LTC4442-1 datasheet, 2007. Available: https://www.analog.com/media/en/technical-documentation/data-sheets/4442fb.pdf

[11] Texas Instruments, Appl. Note SLVA372C. Available: http://www.ti.com/lit/an/slva372c/slva372c.pdf

[12] Microchip, “megaAVR® Data Sheet,” ATmega48A/PA/88A/PA/168A/PA/328/P datasheet, 2018. Available: http://ww1.microchip.com/downloads/en/DeviceDoc/ATmega48A-PA-88A-PA-168A-PA-328-P-DS-DS40002061A.pdf

[13] Arduino, “Adjusting PWM Frequencies” Playground.arduino.cc, 2018. [Online]. Available: https://playground.arduino.cc/Main/TimerPWMCheatsheet [Accessed 15-Oct-2018]

[14] “Turbine Components.” [Online]. Available: http://mstudioblackboard.tudelft.nl/duwind/Wind%20energy%20online%20reader/Static_pages/Cp_lamda_curve.htm [Accessed 16-Oct-2018]]

# Appendix A Requirement and Verification Tables

| Requirements | Verification |
|---|---|
| 1. Wind sensor accurate within 10 %<br>2. RPM Sensor module accurate within 5 %<br>3. Anemometer should be able to function in the rain<br>4. Hall effect sensor enclosure should be IP65 water resistant | 1. (a) Setup the weather station with anemometer located in the power lab. Connect the purchased anemometer to our microcontroller PCB. Program it to determine the wind speed based on the output voltage.<br>(b) Use compressed air from a 1 meter distance aimed at both anemometers. Record the wind speed determined from each anemometer after 3 seconds of compressed air and compare.<br>2. (a) Attach a magnet to the end of a rod attached to a dynamometer.<br>(b) Set up the hall effect sensor to measure when the magnet passes by and connect its output to our microcontroller PCB.<br>(c) Run the dynamometer at 100RPM. Calculate the frequency with the microcontroller based on the hall effect sensor output and compare it to 100RPM to verify 5% accuracy.<br>3. (a) Measure the anemometer's output while using compressed air to spin it<br>(b) Use a spray bottle from 6 inches away to shower the anemometer with water for 1 minute<br>(c) Verify that the measurements are still received by an arduino<br>4. (a) Fill the hall effect sensor enclosure with a dyed anhydrous powder<br>(b) Use a spray bottle from 6 inches away to shower the enclosure with water from all directions for 2 minutes<br>(c) Check the enclosure for any dyed liquid. |

| Requirements | Verification |
|---|---|
| 1. When current is detected by our current sensor, an LED should start blinking | 1. (a) Connect the LED warning circuit to our microcontroller PCB and our current sensor to a simple series resistor circuit capable of dissipating 1 A<br>(b) Program the microcontroller to calculate current from our current sensor output voltage<br>(c) Turn on the power supply and measure the time elapsed with a stopwatch before the LED starts blinking |

| Requirements | Verification |
|---|---|
| 1. Produces a DC output voltage with ripple below 20 % of average voltage at 100 RPM and 400 RPM<br>2. Efficiency >92 % by minimizing conduction loss of the diodes | 1. (a) Connect the PMA outputs to our rectifier circuit, and the output of the rectifier to a power resistor. Connect oscilloscope probes to the power resistor.<br>(b) Use the dynamometer to run the PMA at 100 RPM and 400 RPM<br>(c) Observe the output waveforms on the oscilloscope and confirm the ripple requirement<br>2. Connect power meters to the PMA output using the two wattmeter method and the load. Repeat the above test. |

| Requirements | Verification |
|---|---|
| 1. Output RMS voltage between 23-29 V<br><br>2. Output voltage ripple from DC/DC converter ±3 % of the output voltage at 100 W, ±10 % at 800 W<br><br>3. Efficiency of just the DC/DC converter >80 % at 800 W, >90 % at 100 W | Test the buck-boost converter in the buck mode of operation and the boost mode.<br><br>Buck Mode<br>With a 64 V DC power supply as the input, set the duty ratio to be 0.27. Connect power meters to the input and output. Start with a higher resistance load and slowly decrease the resistance to increase the power at the load.<br><br>1. Use an oscilloscope to measure the output voltage ripple<br><br>2. Use an oscilloscope to measure the RMS output voltage<br><br>3. Use the power meters at the input and output to measure the efficiency.<br><br>Boost Mode<br>Repeat steps 1 - 3 with a 12 V DC power supply as the input, set the duty ratio to be 0.67. |

| Requirements | Verification |
| --- | --- |
| 1. Can calculate the efficiency of the overall system by using the output power read by the voltage and current sensors and the input power calculated from the wind speed<br><br>2. Uses an iterative algorithm to determine the optimal duty ratio for the DC/DC converter to achieve the optimal amount of output power, which is calculated from the current sense resistor and the voltage sensor at the load. The delay should be below 1 second. | 1. (a) Blow compressed air on the anemometer<br>(b) Supply 10 V to a simple resistor divider circuit with attached voltage and current sensors with the load dissipating approximately 20W of power.<br>(c) Program the microcontroller to print out the efficiency computation based on the wind speed and measured voltage and current.<br><br>2. (a) Add a test-point to the hall-effect sensor and a test point to the duty ratio output of the microcontroller.<br>(b) Have the hall effect sensor triggered by a magnet passing by the sensor at 100 RPM (by matching with a metronome) for 30 seconds<br>(c) Change the speed of the magnet passing by the sensor to 50 RPM and measure the time it takes between the hall effect sensor output changing to 50 RPM and the duty ratio changing using an oscilloscope connected to both test points to ensure the output changes within 1 second of the speed changing.<br><br>3. (a) Connect the LCD display to the microcontroller<br>(b) Output test data to the display and ensure it's readable |

| Requirements | Verification |
|---|---|
| 1. Voltmeter capable of measuring the output voltage level within 2 %<br><br>2. Current sensor capable of measuring the output current within 2 % | 1. Measure the voltage of a simple series resistor divider circuit with our voltage sensor connected an arduino. Compare to values determined by the voltage sensor with the value calculated by using the resistances and voltage. Difference should be less than 2 %. Confirm the calculations and measurement with a digital multimetere.<br>(a) Repeat the test with the voltage sensor connected to the microcontroller PCB to verify the interface with our control subsystem<br><br>2. Measure the current of a simple series resistor circuit with our current sensor connected to our microcontroller. Compare to values determined by the current sensor with the value calculated by using the resistance and voltage. Difference should be less than 2 % |

| Requirements | Verification |
|---|---|
| 1. Resistance between 0.9 and 0.95 Ω<br><br>2. Rated for at least 1 kW | 1. Measure the resistance of the resistor bank using a digital multimeter. Record result in lab notebook and verify it is within 5 % of the expected quantity<br><br>2. See power ratings on each resistor or look at their datasheets. Determine the power dissipated by each resistor and verify that no power rating is violated |

## Appendix B AC/DC Converter PCB Layout

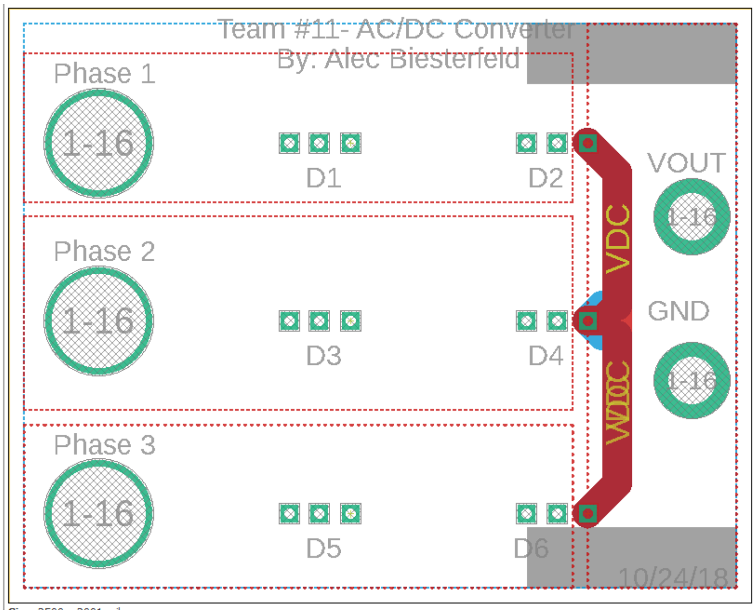

## Appendix C DC/DC Converter PCB Layout

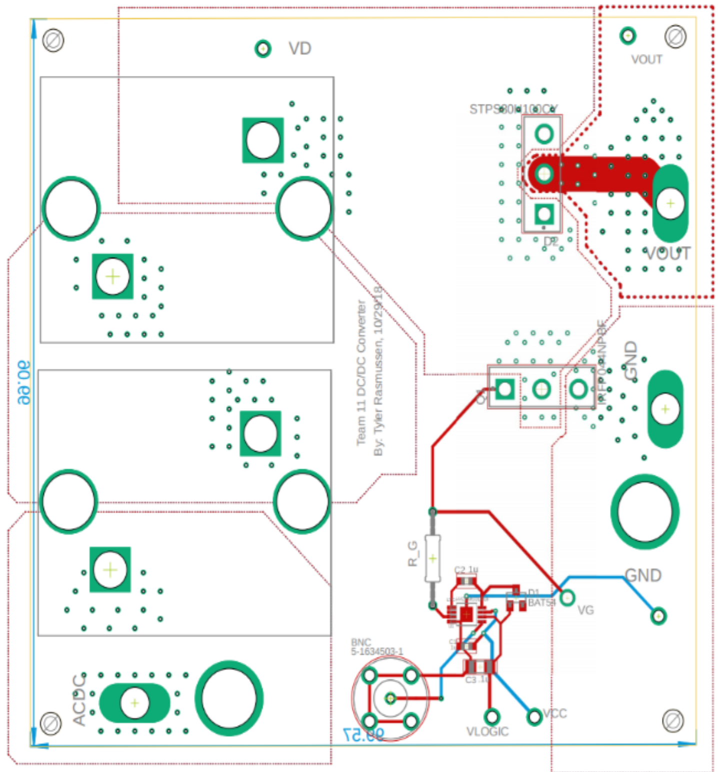

## Appendix D Control System PCB Layout

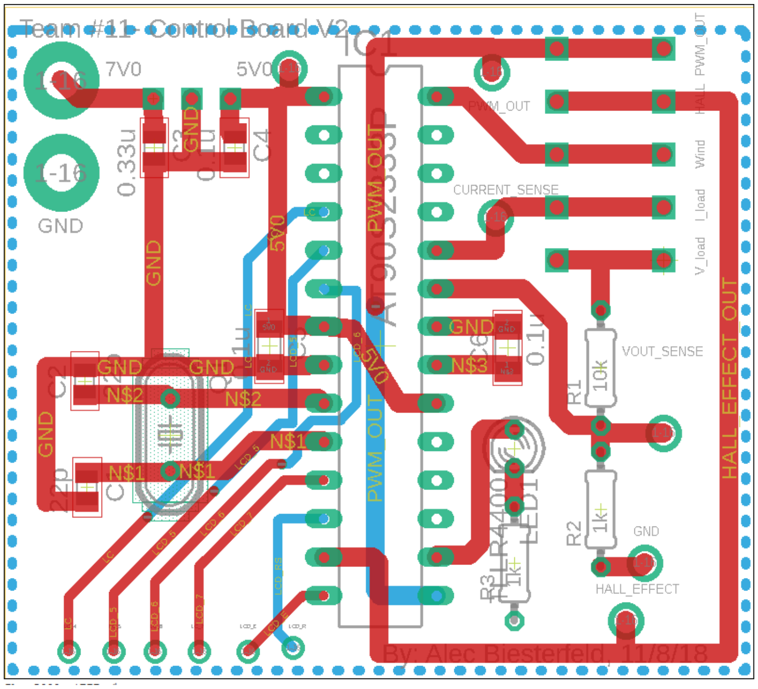

## Appendix E Microcontroller Pinout Table

| Pin Number | Pin Name | Design Function |
|---|---|---|
| 4 | PD2 | LCD Display |
| 5 | PD3 | LCD Display |
| 6 | PD4 | LCD Display |
| 11 | PD5 | LCD Display |
| 12 | PD6 | LCD Display |
| 13 | PD7 | Hall-Effect Sensor Output |
| 14 | PB0 | LCD Display |
| 15 | PB1 | DC/DC Converter PWM signal |
| 16 | PB2 | LED Warning Light |
| 23 | ADC0 | Voltage Sensing |
| 24 | ADC1 | Current Sensing |
| 28 | ADC5 | Wind Sensing |

# Appendix F Schedule

| Week | Tyler | Ben | Alec |
|---|---|---|---|
| 10/8/18 | Buck-boost topology calculations and simulations | Preparing for design review | Compile a list of parts to meet our design specification. Order parts for low voltage and control system components. |
| 10/15/18 | SEPIC converter simulation, help select components for SEPIC converter | Review controls system | Design Microcontroller PCB schematic and layout. Pass audit for PCBway. |
| 10/22/18 | Control system modeling | Look into PID control. | Work on software design. Test progress on a development board. |
| 10/29/18 | Schematic and layout of SEPIC converter | Find transfer function for controls system | Test 1st pass control PCBs. Rework as needed. |
| 11/5/18 | Solder and test SEPIC PCB | Examine relationship between power and voltage | Finish design of second pass PCBs for the control subsystem. Order any additional parts for the second pass. |
| 11/12/18 | Calculations for boost converter, create new PCB | Find relationship between voltage and RPM | Test the second pass control system board. Verify sensor component operations |
| 11/19/18 | Solder and test boost PCB | Assemble controls block diagram | Tune the control algorithm and prepare for system integration. |
| 11/26/18 | Integration testing on the dynamometer, integration testing with the fan | Simulate controls block diagram and boost converter | Debug control algorithm. Implement additional filtering for the power data. |
| 12/3/18 | Tuning algorithm and running tests to prove its operation | Presentation | Prepare system for final demonstration. Collect data to verify our design. |
| 12/10/18 | Presentation and final paper preparation | Final paper | Work on presentation and final paper. |